INSTITUTE OF PHYSICS PUBLISHING NANOTECHNOLOGY
Nanotechnology **17** (2006) 3662–3667 doi:10.1088/0957-4484/17/15/007

A hybrid organic–inorganic electrode for enhanced charge injection or collection in organic optoelectronic devices

Omer F Yilmaz, Sumit Chaudhary and Mihrimah Ozkan[1]

Department of Electrical Engineering, University of California, Riverside, CA 92521, USA

E-mail: mihri@ee.ucr.edu

Received 10 May 2006
Published 27 June 2006
Online at stacks.iop.org/Nano/17/3662

Abstract

Here we report a novel hybrid organic–inorganic anode for organic light-emitting diodes (LEDs) and photovoltaic (PV) cells. This hybrid anode structure is realized from a composite of poly(3,4-ethylene dioxythiophene) doped with polystyrenesulfonic acid (PEDOT:PSS) and indium tin oxide (ITO) nanoparticles. Owing to the phase separation, this anodic structure leads to a graded work function from patterned ITO to the photoactive polymer, which in turn reduces the barrier height for holes by ∼70%. The resulting devices based on this design show up to 67% reduction in turn-on voltage (for polymer LEDs) and up to 40% increase in short-circuit current and power conversion efficiency (for PV cells). Current–voltage characteristics, Fowler–Nordheim analysis, SEM imaging and energy band diagram analysis are employed to characterize the improved performance of our devices. The reported approach is expected to be immensely useful for the molecular design of next-generation efficient organic devices.

(Some figures in this article are in colour only in the electronic version)

1. Introduction

Conjugated polymer-based systems have drawn tremendous attention for optoelectronic applications due to their tunable optical properties, solution processibility, low cost and promising large area fabrication on flexible substrates [1, 2]. Polymer light-emitting diodes (PLEDs) are already occupying their niche in the market next to their inorganic counterparts. On the other hand, PV cells based on polymers are still trying to reach at least the >10% power conversion efficiency requirement for commercialization [3]. Overall, both kinds of devices are basically diodic structures fabricated in the form of a photoactive layer sandwiched between two dissimilar electrodes, one of which needs to be transparent for light transmission. Electroluminescence (EL) in PLEDs is achieved by carrier injection to the polymer chain from both electrodes proceeding by radiative recombination from self-localized excited states [4]. PV cells work in the reverse manner, i.e. an electron–hole pair is generated by optical excitation and subsequently dissociated and collected at the respective electrodes. Hence, balanced charge injection and collection at the electrodes plays a crucial role in the performance of PLEDs and PV cells, respectively [5, 6]. ITO is the most widely used transparent electrode for the organic devices. However, ITO is a non-stoichiometric material which leads to dependence of its electronic properties on the preparation and cleaning methods employed (work function of ITO, $\Phi_{ITO} \sim 4.5$–5.0 eV) [7]. Moreover, due to its high roughness, the devices are likely to have short circuits. In devices with direct contact of ITO to photoactive polymer, it acts as an oxygen and metal ion source, alternating the polymer and resulting in metallic quenching sites for EL [8]. In order to minimize these effects, an intermediate hole injection layer (HIL) (and preferably electron blocking) between the ITO and the photoactive layer is required. Various studies of utilizing conducting polymer films such as polyaniline, polypyrrole, PEDOT as an efficient hole injection layer (HIL) on the transparent, conductive indium tin oxide (ITO) have been reported [9–12]. These polymers not only facilitate hole injection with higher work functions than ITO, but also decrease the dentation of

[1] Author to whom any correspondence should be addressed.

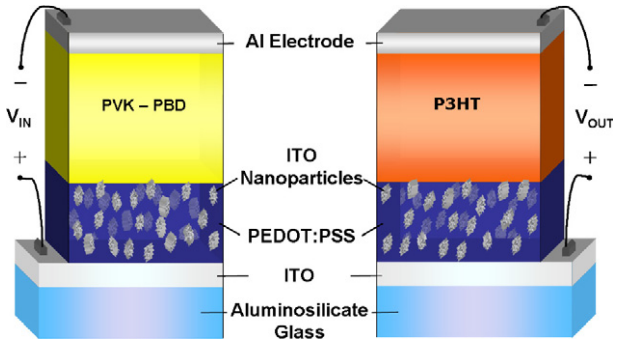

Figure 1. Schematic illustration of the fabricated devices. PVK:PBD is used as the photoactive layer for the LEDs and P3HT is used for the PV cells. ITO nanoparticles are embedded in PEDOT:PSS layer at different concentrations (2% and 5%) to investigate the concentration dependent charge injection/collection in LEDs/PV cells.

the ITO electrode and improve the efficiency and lifetime of the devices. Other studies regarding the modification of transparent electrode with a HIL involve increasing the surface area of the HIL for enhanced hole injection [13] and incorporation of other materials such as perfluorinated ionomers [14] in the PEDOT:PSS matrix. Molecular-scale layered depositions of HIL materials have also shown that further improvements in the efficiency can be achieved with the existing conjugated polymer systems. Ho *et al* [15] reported that the layered deposition results in a graded band structure within the HIL layer significantly increasing the charge injection and external quantum efficiency. Among these, the widely used PEDOT:PSS has become very popular, which is now commercially available, as it is yielding higher efficiencies and increased lifetimes when used as a HIL [16].

Here, we introduce a novel HIL realized from spin coated aqueous solution of PEDOT:PSS incorporated with ITO nanoparticles. Different concentrations of the ITO nanoparticles were embedded in PEDOT:PSS and it was observed that hole injection and collection can be enhanced in PLEDs and PV cells, respectively, based on the aforementioned composite organic–inorganic electrode. By virtue of better charge injection (PLEDs) or collection (PVs), these devices showed better performance than control devices based on the layer of PEDOT:PSS itself spin coated on glass with patterned ITO or control devices that are directly deposited on glass patterned with ITO without PEDOT:PSS. The PEDOT:PSS–ITO nanoparticle electrode combines the advantages of higher work function (∼5.1 eV [16]) of PEDOT:PSS with the low resistance of ITO nanoparticles. These ITO nanoparticles are distributed in the PEDOT:PSS matrix in a graded fashion due to phase segregation, as discussed later in this manuscript. The PLED and PV devices fabricated for the study of the positive electrode are depicted in figure 1.

2. Experimental details

ITO-deposited aluminosilicate glass slides (Delta Technologies Inc., $R_{\text{sheet}} \sim 5$–$15\ \Omega/\square$) were chosen as the substrates. They were etched in 6 M HCl to obtain three 2 mm wide ITO lines with 2 mm spacing. Prior to cleaning, the patterned ITO lines were partially etched by sonication in 1 M HCl in order to remove the short-circuit enhancing dentation of patterned ITO and to obtain a sheet resistance of 40 $\Omega/\square$. The slides were cleaned by ultrasonication in detergent, DI water, trichloroethylene, acetone and isopropyl alcohol, sequentially. The slides were then blow dried with dry nitrogen and kept under vacuum. Just before device fabrication, further cleaning was done by exposure to oxygen plasma for 10 min. PEDOT:PSS was obtained from H. C. Starck (BAYTRON® P VP AI 4083) and filtered through a 0.2 μm PTFE filter (Millipore). ITO nanoparticle suspension in isopropyl alcohol (1.2 g ml^{-1}) with mean diameter size of 25–40 nm was obtained from Aldrich. The suspension was diluted ten times with isopropyl alcohol and sonicated for 12 h to disintegrate the aggregates and then filtered through syringe driven 0.2 μm filter. Next, PEDOT:PSS solutions containing 2% and 5% ITO nanoparticles by volume were prepared with the assistance of 15 min of sonication at 40 °C, followed by sheer mixing for 1 h. PEDOT:PSS and ITO nanoparticles were observed to be well dispersed in the final mixture by virtue of pristinely hydrophilic aqueous and isopropylic solutions, respectively. There was no significant phase separation in solution form with even higher concentration of ITO nanoparticles in PEDOT:PSS. These PEDOT:PSS–ITO nanoparticle suspensions were spin coated on the aluminosilicate slides in a nitrogen environment with a speed of 1000 rpm for two minutes resulting in a typical thickness of 80 nm confirmed by a Hyphenated Systems 3D Confocal Microscope (results not shown). The spin coated slides were prebaked on the hot plate at 110 °C for 5 min and this was followed by storage in vacuum oven at 60 °C for 1 h. For PLEDs, the hole conducting poly(*n*-vinylcarbazole) (PVK) and electron conducting oxidiazole derivative 2-(4-biphenylyl)-5-phenyl-1,3,4-oxidiazole (PBD) were mixed in a 2:1 weight ratio to result in a 15 mg ml^{-1} solution in chloroform, and then spin coated to form the electroluminescent film above the anodes with an approximate thickness of 80 nm. On the other hand, the PV cells were fabricated with a 17 mg ml^{-1} solution of poly(3-hexylthiophene (P3HT) in 1,2-dichlorobenzene spin coated at 800 rpm for 1 min giving a film thickness of approximately 200 nm. After drying the devices at 70 °C in nitrogen purged oven for 2 h, the aluminium electrodes were evaporated with shadow masking method under a vacuum of 10^{-6} mbar. Resulting devices with active areas ∼4 mm^2 were tested in the ambient atmosphere. Current–voltage (I–V) characteristics were obtained with an Agilent HP4155C Semiconductor Parameter Analyzer. EL of the PLEDs was collected in the Perkin-Elmer LS 55 Luminescence Spectrometer and photovoltaic devices were illuminated by a 50 W halogen bulb with a light intensity of 50 mW cm^{-2} on the device plane. A Leo Supra 55 scanning electron microscope was used for cross-sectional imaging of the PEDOT:PSS–ITOnp electrode.

Control devices were also prepared containing only PEDOT:PSS film as the HIL for both PLED and PV devices. An additional control device without any PEDOT:PSS layer was also prepared with the same method. For simplicity of discussion in the rest of the communication, characterized devices here will be referred as ITO, PEDOT:PSS, PEDOT:PSS–ITOnp2 and PEDOT:PSS–ITOnp5 for devices with only prepatterned ITO, PEDOT:PSS

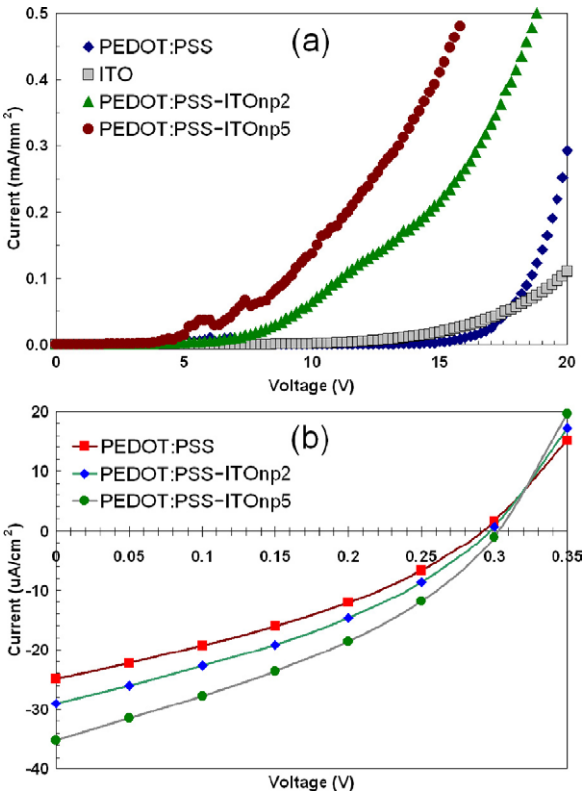

Figure 2. I–V characteristics of the (a) PLEDs and (b) PV cells. (a) The turn-on voltage reduces and in (b), short-circuit current increases for the case of electrodes employing PEDOT:PSS–ITO nanoparticle composite.

above prepatterned ITO and PEDOT:PSS with 2% and 5% ITO nanoparticles, respectively.

3. Results and discussion

The effect of ITO nanoparticle concentration in the PEDOT:PSS layer on the I–V characteristics of the devices is shown in figure 2. For the PLED configuration with the active layer of PVK–PBD the evolution of the threshold voltage for different HIL is depicted in figure 2(a). The PEDOT:PSS device showed a threshold voltage around 15 V, with a turn-on voltage of ∼16 V. With the addition of ITO nanoparticles, the threshold voltages of the diodes are significantly reduced to 8 V (47%) and 5 V (67%) for PEDOT:PSS–ITOnp2 and PEDOT:PSS–ITOnp5, respectively. The decrease in the threshold voltage (47–67%) suggests easier carrier injection from the positive electrode. For further investigation, another I–V characteristic of the ITO-only device (ITO/PVK–PBD/Al) is also shown in figure 2(a). The threshold voltage of this device is around 13 V, with a turn-on voltage of ∼15 V. However, the maximum current achievable in this configuration is the lowest.

The EL spectra of these devices at the same applied voltage (not shown) indicate that the lowest emission is from ITO/PVK–PBD/Al device, followed by the one with the PEDOT:PSS layer above prepatterned ITO. The PEDOT:PSS–ITOnp2 and PEDOT:PSS–ITOnp5 devices did not show a significant change in the EL intensity compared with the device with PEDOT:PSS only. However, further increase in the ITO nanoparticle concentration resulted in a decrease in their illumination, which suggests an increase of nanoparticle population in the surface of PEDOT:PSS layer leading to quenching of excitons before radiative recombination. At the same time, electron injection from the negative electrode was another constraint on the electric field induced emission [5]. Hence, the resulting increase in current in devices with high concentrations of ITO nanoparticles does not contribute to emission which is most possibly caused due to an unbalanced carrier injection from the respective electrodes. This observed increase in current, then, can be explained by only the increase of hole injection from the positive electrode. As a result of that, the lack of increase of illumination in case of PEDOT:PSS–ITOnp2 and PEDOT:PSS–ITOnp5 is not surprising as enhanced electron injection from the cathode would be required for higher recombination efficiencies. Nevertheless, if equivalent improvements are made on the cathode side [17], our results still provide insights into further pushing the limits of the anodic side for more efficient PLEDs.

Figure 2(b) shows the I–V characteristics of the PV cells under illumination. The open circuit voltage, V_{oc}, is around 0.3 V, which is consistent with metal–insulator–metal diode model, resulting from the difference of anode and cathode work functions (Al ∼ 4.3 eV [18]). There is a significant increase in the short-circuit current, I_{sc}, of the devices with increasing concentration of the ITO nanoparticles. The I_{sc} for the PEDOT:PSS device was around 25 μA cm^{-2}, whereas it was measured as 29, and 35 μA cm^{-2} for PEDOT:PSS–ITOnp2 and PEDOT:PSS–ITOnp5 devices, respectively. This change in the electrode shows facilitated hole collection at the anode. The fill factors (FF) of the devices are 33%, 33.5% and 34% which remain mostly unchanged. The devices were not annealed and no postfabrication treatment was applied. It was reported by many researchers that annealing has increasing effects in both I_{sc} and FF [19]. It should be noted that the PV devices were prepared for the relative investigation of the anodes, not to achieve the highest efficiency PV system. The I–V characteristics of these devices are shown for the purpose of illustrating the evolution of the performance of the diode under illumination. Here, the effect of ITO nanoparticles introduces a remarkable increase in the I_{sc} (16% and 40% for PEDOT:PSS–ITOnp2 and PEDOT:PSS–ITOnp5, respectively), which increases the power conversion efficiency of the PV cell as it is directly proportional to I_{sc} for constant V_{oc} and FF.

The enhanced charge injection (or collection for the PV cells) is mainly due to presence of the highly conductive ITO nanoparticles in the PEDOT:PSS layer. PEDOT:PSS has a higher resistivity (500–5000 Ω cm [16]) with respect to ITO. Incorporation of ITO nanoparticles in the PEDOT:PSS layer basically makes the positive electrode more conductive resulting in easier carrier transport. In addition to this, due to the high surface area of nanoparticles [20] in the polymer matrix, carrier transport is facilitated in three dimensions within HIL. To understand the effect of incorporation of ITO nanoparticles in the PEDOT:PSS network, we analysed the I–V characteristics of the PLEDs with the Fowler–Nordheim tunnelling theory [5]. Previous studies have shown good

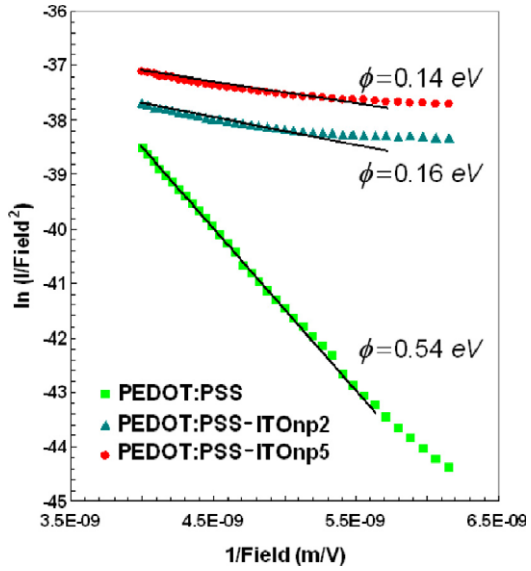

Figure 3. Fowler–Nordheim plots for ITO/HIL/PVK–PBD/Al devices with electrodes of 2% and 5% ITO nanoparticle concentrations in PEDOT:PSS. For comparison, similar data for the control device ITO/PEDOT:PSS/PVK–PBD/Al are also obtained.

agreement with this theory [5, 6, 11, 13]. Fowler–Nordheim field emission tunnelling theory predicts that [21]

$$I \propto F^2 \exp\left(-\frac{\kappa}{F}\right), \tag{1}$$

where I is the current, F is the electric field strength and κ is a parameter that depends on the shape of the barrier at the metal–polymer contact. If we assume that tunnelling current is through a triangular barrier at the positive electrode interface, the κ in equation (1) is given by [22]

$$\kappa = \frac{8\pi\sqrt{2m^*}\phi^{3/2}}{3qh}. \tag{2}$$

In equation (2), ϕ is the height of the barrier, m^* is the effective mass of the holes in the PVK–PBD complex and h is Planck's constant. Here, equation (2) assumes that the electric field is constant across the device and the effective mass equal to the free electron mass [5]. The discussed PLED devices could also be approximated as hole-only devices since there exists a high barrier at the polymer/Al interface (Φ_{Al}: 4.3 eV, electron affinity (EA), EA_{PVK}: 2.2 eV, EA_{PBD}: 2.6 eV [23, 24]). Our experiments showed consistent increase in the current with increasing concentration of the ITO nanoparticles. Figure 3 shows a plot of $\ln(I/F^2)$ versus $1/F$ for ITO/PEDOT:PSS–ITOnp/PVK–PBD/Al devices and the PEDOT:PSS control device fabricated with an approximate active layer thickness of 80 nm. The effective barrier heights were calculated using equations (1) and (2). The barrier of the PEDOT:PSS layer device was found to be 0.54 eV without the ITO nanoparticles. With the introduction of the ITO nanoparticles in the PEDOT:PSS network, the barrier was reduced to 0.16 eV (70%) and 0.14 eV (74%) for 2% and 5% volume concentrations, respectively. It seems evident that barrier reduction is the most plausible factor behind the improved performance of our PLEDs and PV cells.

Besides the energetic arguments behind the observed results, a question arises about the physical/morphological nature of our hybrid PEDOT:PSS–ITOnp electrode and its implications for the aforementioned observations. Hence, for further elucidation, we obtained SEM images of the PEDOT:PSS–ITOnp electrodes, which are shown in figure 4, along with the schematic illustration of the observed distribution of ITO nanoparticles across the PEDOT:PSS layer. It was observed that due to the dissimilar chemistry of inorganic ITO nanoparticles and organic PEDOT:PSS, phase segregation occurs and ITO nanoparticles tend to settle down upon spin coating even though the original solution mixture was highly uniform. Cross-sectional SEM images in figure 4 illustrate this phenomenon. A similar phenomenon has been observed before for polymer and nanoparticle systems owing to mass and chemistry differences between the two [25]. In the surface SEM images and upper part of cross-sectional SEM images, no ITO particles were observed. This phenomenon is functionally advantageous as it leads to a graded work function values from patterned ITO on glass, to regime dominated by ITO nanoparticles and finally to the regime dominated by PEDOT:PSS. Hence, the holes are smoothly transferred to the PEDOT:PSS layer without having an offset at the ITO electrode–PEDOT:PSS interface because of the spatial distribution of the ITO nanoparticles. Even though the device was prepared with 5% ITO nanoparticle solution

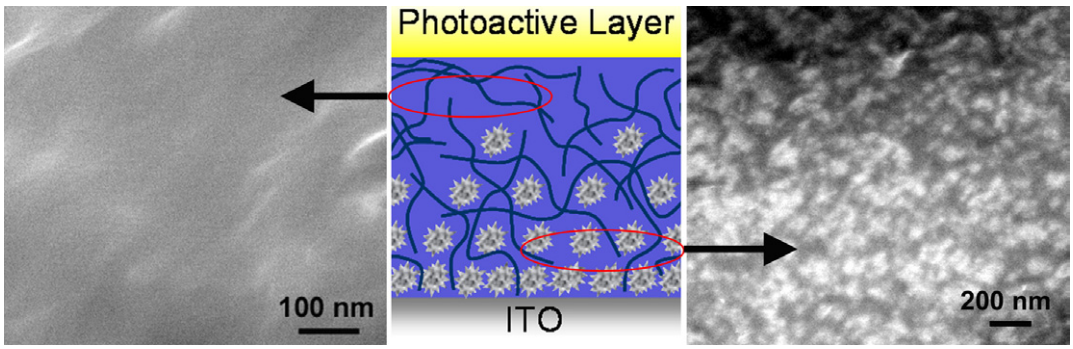

Figure 4. Schematic (middle) and SEM illustrations (left and right) of the phase separation between organic PEDOT:PSS and inorganic ITO nanoparticles. The left image shows the PEDOT:PSS (in the schematic diagram, lines represent polymer chains), which predominates at the top edge of the hybrid organic–inorganic electrode layer. ITO nanoparticles tend to settle down on spin coating and are shown in the cross-sectional image on the right. No nanoparticles were observed on the top region of the cross-sectional image.

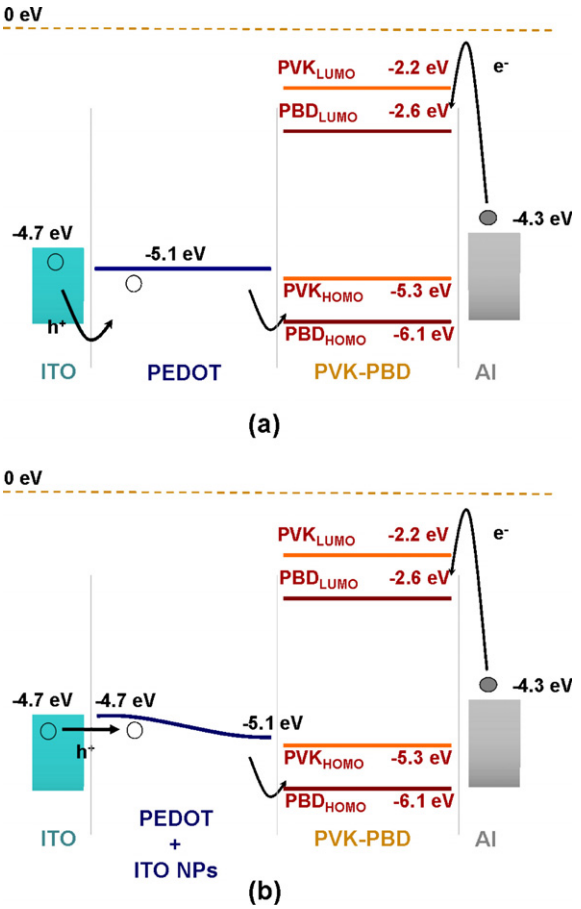

Figure 5. The band diagram of the fabricated OLEDs: (a) control device with only PEDOT:PSS as the HIL. There exist two barriers for the holes when the positive bias is applied: first at the ITO electrode–PEDOT:PSS interface and second at the PEDOT:PSS–polymer complex interface. (b) The devices with ITO nanoparticles embedded in the PEDOT:PSS matrix. The phase separation in the HIL layer between the ITO nanoparticles and PEDOT:PSS results in a smooth transition from the energy level of the ITO (−4.7 eV) to the PEDOT:PSS (−5.1 eV). Hence, when the positive bias is applied the barrier at the ITO electrode–PEDOT:PSS interface is eliminated.

which would be lower than the percolation threshold, the phase separation suggests that the ITO nanoparticle concentration is much higher than 5% at this interface which can be predicted at the percolation threshold or above. Therefore, the discussed transition from the ITO electrode's energy state to PEDOT:PSS's energy state is particularly removing the offset which was creating a triangular barrier of height 0.4 eV when a positive bias is applied. For the control device the total barrier that the holes experience is 0.6 eV as can be seen from figure 5(a). The calculated effective barrier height for the control device in the Nordheim–Fowler regime was 0.54 eV as discussed earlier. The PEDOT:PSS–ITOnp devices with graded bands have only one offset which creates a 0.2 eV barrier at the PEDOT:PSS and PVK–PBD complex as seen from figure 5(b).

The previously calculated effective barrier height 0.14 eV (for PEDOT:PSS–ITOnp5 device) lies in the proximity of the barrier seen from the band diagram. The deviations between the calculated effective barrier height from the experimental data and the suggested barrier height from the band diagrams may be resulting from the discrepancy of the energy levels given in the literature for the materials and the exact energy levels of materials used in our experiments. Besides this, further reduction of the barrier height may also be taking place due to the image charges built in the ITO electrode or ITO nanoparticles in high electric fields in the device which was not taken into consideration in our calculations.

4. Summary

In summary, we have demonstrated that devices with embedded ITO nanoparticles in the PEDOT:PSS network exhibit improved performance over single PEDOT:PSS layer or single inorganic ITO film devices. This includes between 47 and 67% drop in threshold voltage and between 70 and 74% drop in the barrier height for PLEDs, and up to 40% increase in short-circuit current for PV cells. Hence, an obvious total current increase is observed in the I–V characteristics of both PLEDs and PV cells fabricated with ITO nanoparticles. These results are due to the facilitated hole transport in the HIL with the graded 3D morphology of the PEDOT:PSS layer with ITO nanoparticles. The underlying phenomenon is studied by Fowler–Nordheim analysis and it was found out that there is a significant reduction of the effective barrier at the anode/polymer interface. Our method unifies the advantages of higher work function of PEDOT:PSS while maintaining the same optical performance and conductivity of ITO nanoparticles to enhance the carrier transport. Additionally, the incorporation of the ITO nanoparticles is expected to cause increased surface area at the charge transfer interface between PEDOT:PSS and ITO film. This might also have a desirable bearing on the resultant improved characteristics [13]. The performance of both PLEDs and PV cells can further be improved by a similar methodology of modification at the cathode side. It has been shown that the increased surface area of the cathode, controlled by the film drying time, improves the efficiency of the solar cells [26]. The methodology demonstrated by us combined with the improvement on the negative electrode side can further lead to devices with enhanced electrical and optical performance due to balanced charge injection/collection to/from the photoactive layer.

Acknowledgments

We would like to acknowledge our funding support for OFY from Southern California Public Power Agency, and funding support for SC from the Riverside Public Utilities and University of California Energy Institute.

References

[1] Bernius M T, Inbasekaran M, O'Brien J and Wu W 2000 *Adv. Mater.* **12** 1737
[2] Brabec C J, Sariciftci N S and Hummelen J C 2001 *Adv. Funct. Mater.* **11** 15
[3] Brabec C J, Hauch J A, Schilinsky P and Waldauf C 2005 *MRS Bull.* **30** 50

[4] Burroughes J H, Bradley D D C, Brown A R, Marks R N, Mackey K, Friend R H, Burns P K and Holmes A B 1990 *Nature* **347** 29
[5] Parker I D 1994 *J. Appl. Phys.* **75** 1656
[6] Heeger A J, Parker I D and Yang Y 1994 *Synth. Met.* **67** 23
[7] Osada T, Kugler T, Broms P and Salaneck W 1998 *Synth. Met.* **96** 77
[8] Scott J, Kaufman J, Brock P, Dipieto R, Salem J and Goitia J 1996 *J. Appl. Phys.* **79** 2745
[9] Higgins R W T, Zaidi N A and Monkman A P 2001 *Adv. Funct. Mater.* **11** 407
[10] Carter S A, Angelopoulos M, Karg S, Brock P J and Scott J C 1997 *Appl. Phys. Lett.* **70** 2067
[11] Gao J, Heeger A J, Lee J Y and Kim C Y 1996 *Synth. Met.* **82** 221
[12] Elschner A, Bruder F, Heuer H W, Jonas F, Karbach A, Kirchmeyer S, Thurm S and Wehrmann R 2000 *Synth. Met.* **111/112** 139
[13] Yang Y, Westerweele E, Zhang C, Smith P and Heeger A J 1995 *J. Appl. Phys.* **77** 694
[14] Lee T W *et al* 2005 *Appl. Phys. Lett.* **87** 231106
[15] Ho P K H, Kim J, Burroughes J H, Becker H, Li S F Y, Brown T M, Cacialli F and Friend R H 2000 *Nature* **404** 481
[16] Product information for BAYTRON® P VP AI 4083 can be found at http://www.hcstarck.com
[17] Jabbour G E, Kippelen B, Armstrong N R and Peyghambarian N 1998 *Appl. Phys. Lett.* **73** 1198
[18] Michaelson H 1978 *IBM J. Res. Dev.* **22** 72
[19] Li G, Shrotriya V, Yao Y and Yang Y 2005 *J. Appl. Phys.* **98** 243506
[20] Product information for ITO nanoparticle dispersion can be found at http://www.sigmaaldrich.com
[21] Fowler R H and Nordheim L 1928 *Proc. R. Soc.* A **119** 173
[22] Sze S M 1981 *Physics of Semiconductor Devices* (New York: Wiley)
[23] Wu C C, Sturm J C, Register R A, Tian J, Dana E P and Thompson M E 1997 *IEEE Trans. Electron Devices* **44** 1269
Becker H, Burns S E and Friend R H 1997 *Phys. Rev.* B **56** 1893
[24] Chaudhary S, Chan W C W and Ozkan M 2004 *Appl. Phys. Lett.* **84** 2925
[25] Coe S, Woo W, Bawendi M and Bulovic V 2002 *Nature* **420** 800
[26] Li G, Shrotriya V, Huang J, Tao Y, Moriarty T, Emery K and Yang Y 2005 *Nat. Mater.* **4** 864